ELSEVIER

Ceramics International 31 (2005) 839–844

CERAMICS INTERNATIONAL

www.elsevier.com/locate/ceramint

Porcellanite–$CaCO_3$ high temperature reaction: phases, microstructure, microhardness

J.C. Knight

Department of Physics, University of the West Indies, St. Augustine, Trinidad and Tobago

Received 25 June 2004; received in revised form 23 July 2004; accepted 3 September 2004
Available online 25 January 2005

Abstract

The characteristics of reaction phases, microstructure and microhardness of thermally fused powder mixtures of porcellanite and limestone batched in various proportions have been studied after firing at 1200 °C. X-ray diffraction and scanning electron microscopy were employed in phase and microstructure investigation, respectively. Formed as thermo-chemical reaction products, morphologically flat, thin, randomly orientated plates of $3CaO{\cdot}Al_2O_3{\cdot}2SiO_2$ and $2CaO{\cdot}Al_2O_3{\cdot}SiO_2$ embedded in molten $3CaO{\cdot}2SiO_2$ characterized the microstructure of compositions originally containing 60 and 70% porcellanite. In contrast, and consistent with XRD phase identification, the microstructures of the mixtures originally containing 75% and higher porcellanite featured predominantly $3CaO{\cdot}2SiO_2$-bonded particulate and/or dendritic and fibrous mullite. Retained in compositions originally containing $\geq$50% porcellanite, remnant unreacted free silica featured microstructurally as fine dispersed rounded particles. For the compositions which fused sufficiently strongly and homogeneously to facilitate indentation hardness testing (50–90% porcellanite), Vickers microhardness increased through maximum then gradually decreased with increasing porcellanite content.

Keywords: A. Powders: solid state reaction; B. Microstructure-final; C. Hardness

1. Introduction

Suitably proportioned, and fired at sufficiently high temperatures, leucite-rich variants of Trinidad porcellanite and limestone react to form $3CaO{\cdot}2SiO_2$ (C_3S_2), $3CaO{\cdot}Al_2O_3{\cdot}2SiO_2$ (C_3AS_2) and $2CaO{\cdot}Al_2O_3{\cdot}SiO_2$ (C_2AS) [1]. The C_3S_2 reaction results from combination of lime, derived from the limestone, and free silica from the porcellanite, known to be pozzolanic [2,3]. Combination of lime with mullite, a thermo-chemical transformation by-product of leucite [4], gives rise to C_3AS_2 and C_2AS.

When cooled to room temperature, certain compositions fused to dense and hard homogeneous crystalline materials embodying the reaction products. This paper reports on reaction phases formed in mixtures covering the range 10–90% of the porcellanite and limestone after firing at 1200 °C and on the microstructures and microhardness of the compositions, which fused homogeneously.

2. Experimental procedure

Mineralogically, the porcellanite used was comprised principally of leucite, silica and kalsilite, while the limestone was pure calcite, free of dolomite. In terms of chemical composition, X-ray fluorescence (XRF) quantification showed that the major oxides present in the porcellanite were in the amounts: SiO_2, 62.3%; Al_2O_3, 23.9%; Fe_2O_3, 5.8%; K_2O, 3.4%; MgO, 0.6%.

Both raw materials were batched in powdered form (<500 μm particle size) to cover the range 10–90% by weight of one in the other. Compacts of the various mixes were subsequently fired for 2 h at a holding temperature of 1200 °C in an electric furnace heated at 25 °C/min.

Phase analysis of the fired samples (ground to sub-75 μm particle size) was done by X-ray diffraction in a Siemens 5000D diffractometer using Cu Kα radiation. Microstructural study involved secondary electron scanning electron microscopy (SEM) of both fractured sections and polished and chemically etched surfaces in a Phillips 500

E-mail address: jknight@fans.uwi.tt.

0272-8842/$30.00
doi:10.1016/j.ceramint.2004.09.012

microscope. Etching of polished sections was done for 3 s at room temperature (typically 25 °C) using 20% hydrofluoric acid.

Vickers microhardness testing (using a load of 1 kgf) was used to investigate hardness and indenter contact response of the compositions, which fused sufficiently strongly to facilitate satisfactory polishing.

3. Results and discussion

3.1. XRD

Fig. 1 shows normalized XRD profiles of the various porcellanite–$CaCO_3$ mixes after firing at 1200 °C. Also included are the profiles of the porcellanite alone with no added limestone (100 P) and the limestone alone (100 C). Representative peaks, identifying silica, mullite, lime and the reaction products C_3S_2, C_3AS_2 and C_2AS are indicated. While it is evident from relative peak intensities that yield in the reaction products and the amount of free lime, free silica and mullite vary with composition, the trends in variation are best appreciated from Fig. 2. Here it can be seen that within the range of composition in which the individual reaction products formed, indicative yield increases through maximum then decreases with increasing porcellanite content. Free mullite, silica and lime were retained in compositions

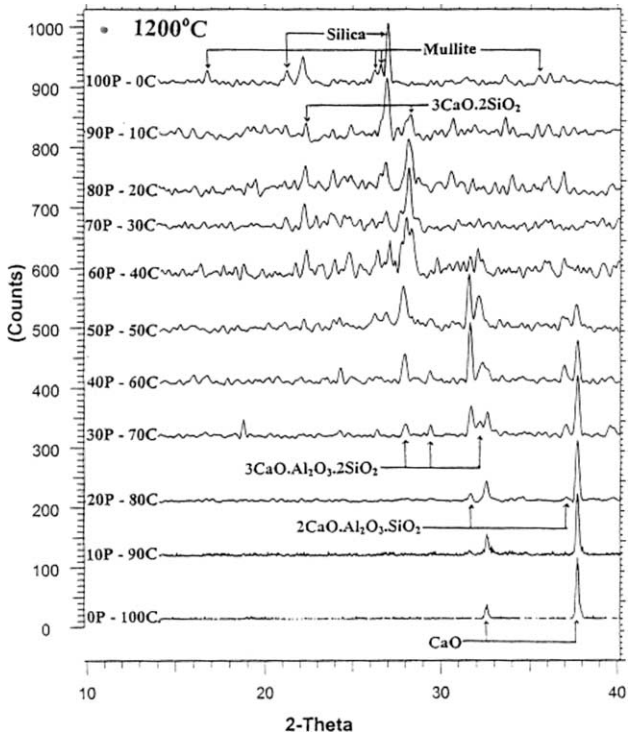

Fig. 1. Normalized XRD profiles of the various compositions after firing at 1200 °C. The designation *X*P–*Y*C means *X*% porcellanite and *Y*% limestone.

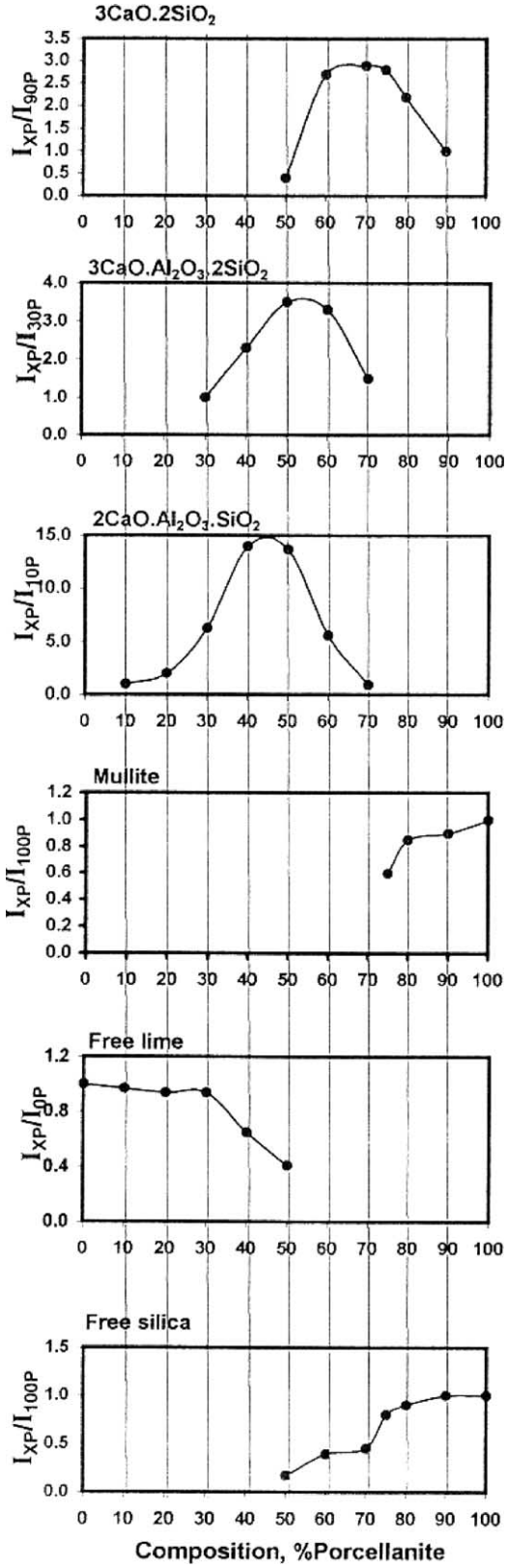

Fig. 2. Indicative amounts of the reaction products, free mullite, silica and lime (as a function of composition) in terms of normalized peak intensity relative to the compositions indicated by subscript in the denominator of I_{XP}/I_{xP}. For the individual compounds the data were compiled from Fig. 1 using the representative peaks cited in Table 1.

Table 1
The representative 2θ peaks of Fig. 1 used to compile the data of Fig. 2

Compounds	Abbreviation	Representative 2θ peak (°)
$3CaO{\cdot}2SiO_2$	C_3S_2	28.3
$3CaO{\cdot}Al_2O_3{\cdot}2SiO_2$	C_3AS_2	28.1
$2CaO{\cdot}Al_2O_3{\cdot}SiO_2$	C_2AS	31.5
Mullite		26.2
Free silica		27.1
Free lime		37.7

originally containing ≥75, ≥50 and ≤50% porcellanite, respectively.

3.2. Microstructure

Meaningful microstructural investigation was possible only for the samples that fused strongly on firing. These spanned the range 50–90% porcellanite in which C_3S_2 was detected (Fig. 2). Known to be in molten state at 1200 °C [1], it is this reaction product which effects strong homogeneous fusing. Consistent with this, C_3S_2 was not detected in compositions originally containing 40% and less porcellanite (due, most likely, to minimal yield on account of the amount of available free silica), which after firing, were weak and crumbly, mitigating against sample preparation for microstructural analysis.

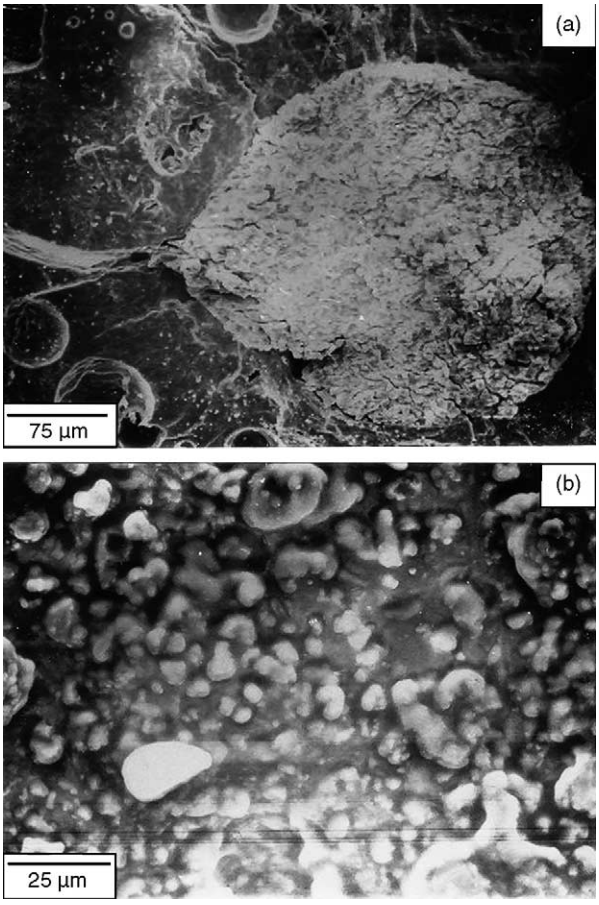

Fig. 3. Secondary electron SEM images of: (a) fractured and (b) polished and etched sections of the sample originally containing 50% porcellanite. Note pocket of slaked lime at right in (a).

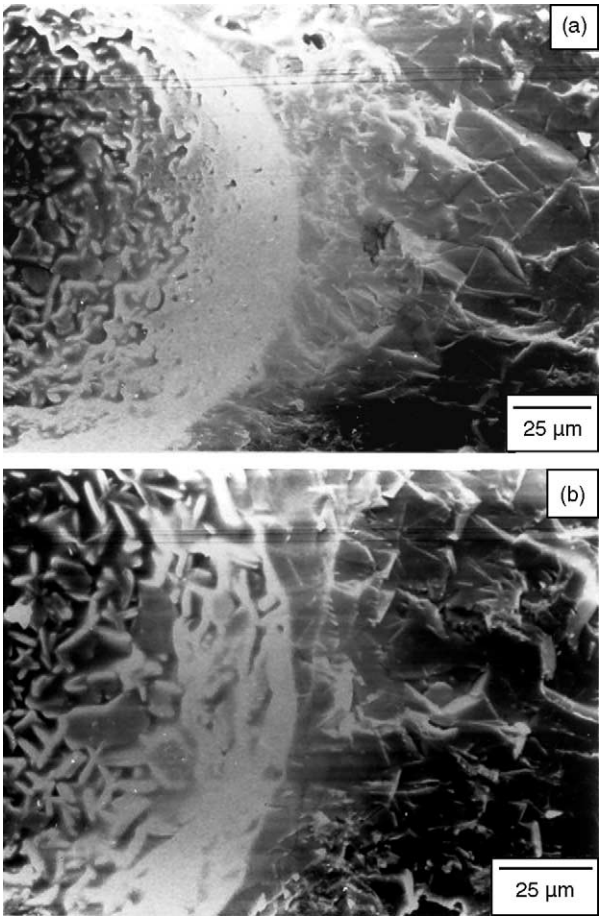

Fig. 4. SEM images of fractured sections of the samples originally containing: (a) 60% and (b) 70% porcellanite. Note distinctly resolved crystals at left in both images.

For the composition originally containing 50% porcellanite, fractured sections featured pockets of unreacted free lime (slaked to $Ca(OH)_2$ by interaction with atmospheric water vapour) interspersed in a dense but microstructurally non-descript major phase (Fig. 3(a)). However, after polishing and etching, fine, rounded, remnant unreacted silica, randomly dispersed in molten C_3S_2, became evident (Fig. 3(b)).

In the case of the compositions originally containing 60 and 70% porcellanite, fine details of microstructure were adequately revealed in fractured sections. In particular, Fig. 4 shows distinctly resolved fine crystals embedded in molten C_3S_2 at exposed crater surfaces which originally interfaced with pockets of free lime. Based on the X-ray information of Figs. 1 and 2, these are identified as crystals

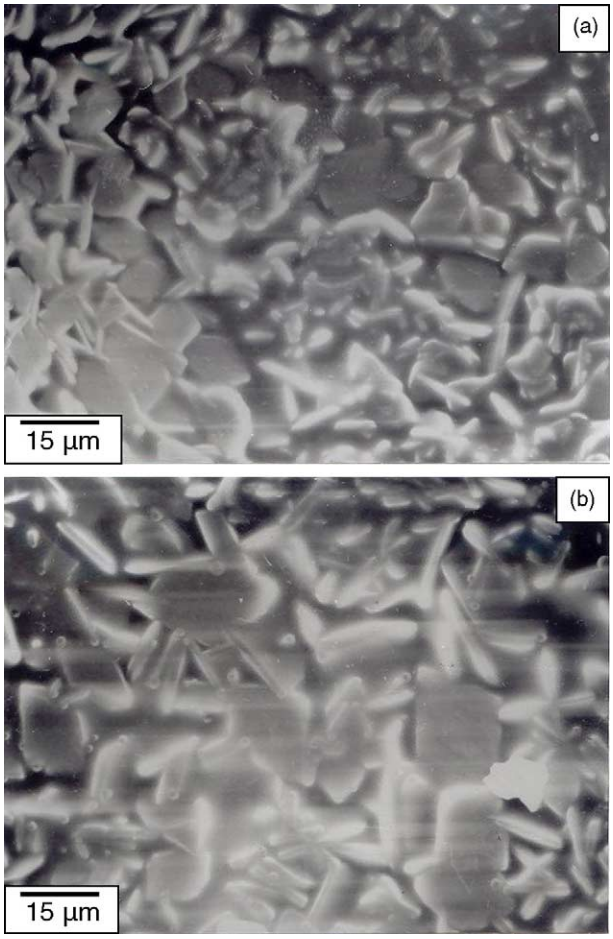

Fig. 5. High magnification SEM images of: (a) and (b), the C_3AS_2 and C_2AS crystals at left in Fig. 4(a) and (b), respectively.

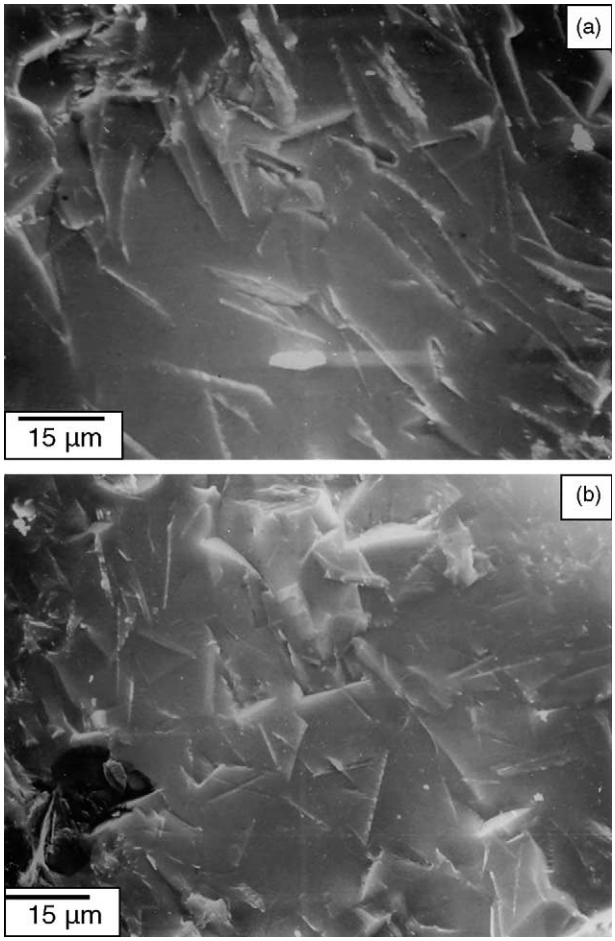

Fig. 6. Typical fracture surface appearance away from the crater areas in Fig. 4(a) and (b), respectively.

of C_3AS_2 and C_2AS. Further, it is evident in Fig. 4, and more so in Fig. 5, that morphologically, C_3AS_2 and C_2AS crystallize predominantly into thin, randomly orientated flat plates, appearing mostly rectangular. However, in addition to rectangular growth, possible hexagonal growth also seems apparent in Fig. 5(a). Outside the crater areas of Fig. 4, general fracture surface appearance (Fig. 6) also reflects the plate structure and random orientation of the C_3AS_2 and C_2AS crystals in the C_3S_2 matrix. In Figs. 4 and 5 remnant unreacted free silica appears as tiny, dispersed, rounded particles.

For compositions originally containing 75, 80 and 90% porcellanite, XRD suggests that the microstructures should feature only C_3S_2, mullite and silica (Figs. 1 and 2). Consistent with this, etched sections of the composition originally containing 75% porcellanite revealed a microstructure characterized mainly by fine particulate and dendritic mullite embedded in C_3S_2 (Fig. 7(a) and (b)). However, although not abundant, isolated strands of long-fibre mullite were also observed (Fig. 7(b) and (c)). For the samples originally containing 80 and 90% porcellanite, no evidence of particulate and dendritic mullite was found. Instead, the microstructure of these compositions, as revealed in etched sections (Fig. 8), featured intricate configurations of long strands of bundled and individual mullite fibres permeating the C_3S_2 matrix. As in the case of the compositions originally containing 50–75% porcellanite, remnant unreacted free silica appears as tiny rounded particles (Fig. 8).

3.3. Microhardness

As with the microstructural investigation, microhardness measurements were possible only for the samples, which fused homogeneously. For these, Fig. 9 shows that Vickers microhardness was lowest for the sample originally containing 50% porcellanite in which the relative amount of bonding phase, C_3S_2, formed was least (Fig. 2). Thereafter microhardness increased through maximum for the sample originally containing 60% porcellanite, then gradually decreased with increasing porcellanite content.

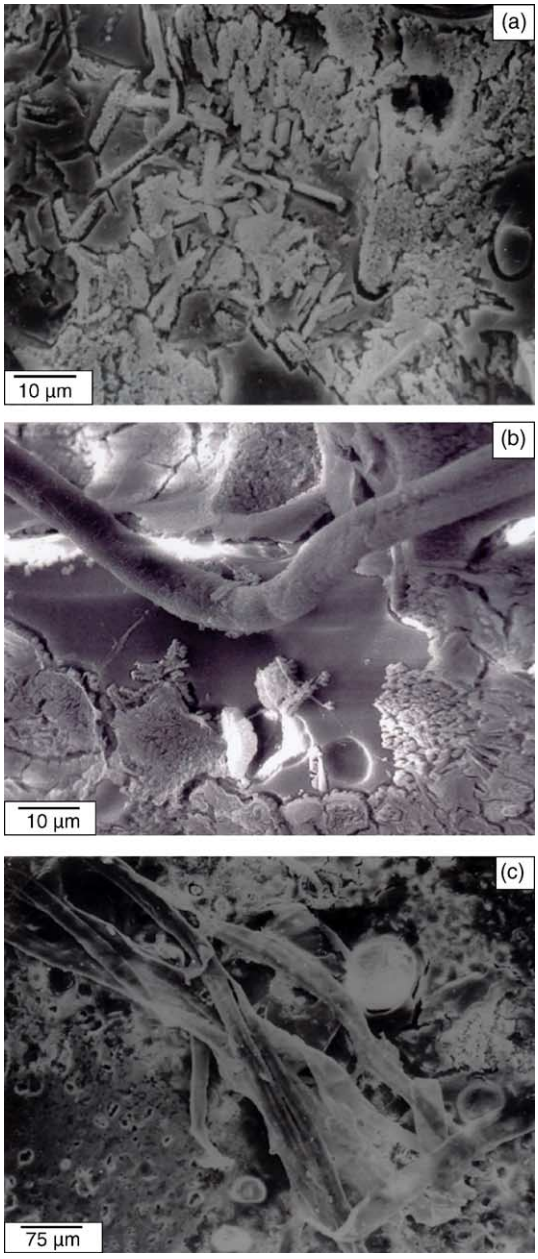

Fig. 7. Etched sections showing mixed mode mullite growth in the composition originally containing 75% porcellanite. In addition to fine particulate and dendritic growth ((a) and (b)), long-fibre growth ((b) and (c)) also occurred.

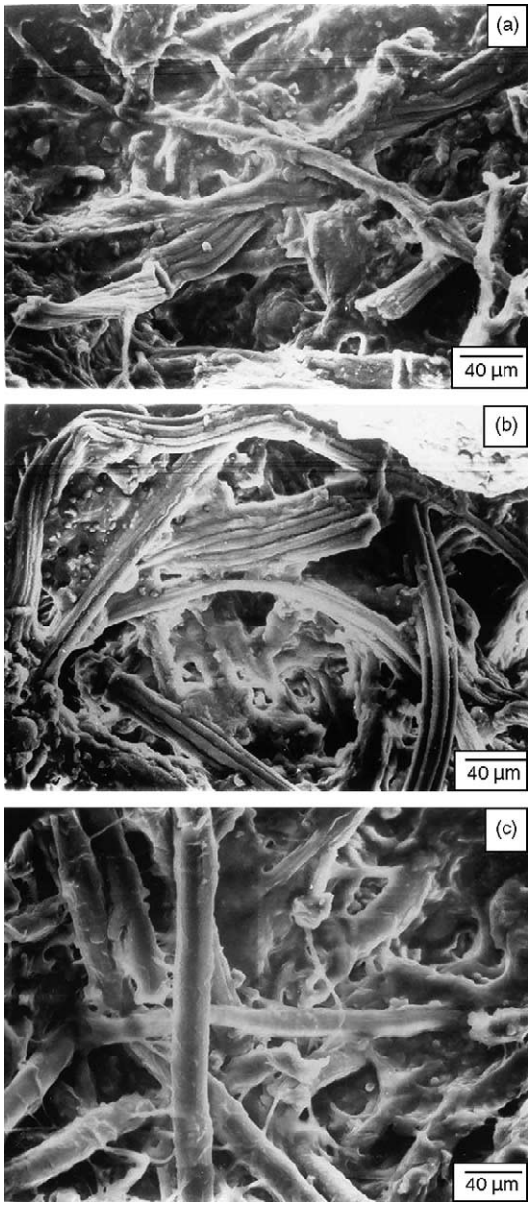

Fig. 8. Etched sections showing intricate configurations of bundled and single mullite fibres permeating the C_3S_2 matrix of the samples originally containing: ((a) and (b)) 80% and (c) 90% porcellanite.

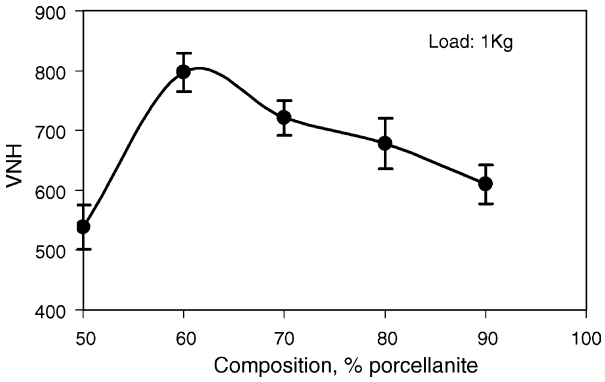

Fig. 9. Vickers hardness number (VHN) as a function of composition.

Regarding indenter contact response, all the samples exhibited radial cracks (Fig. 10), typical of Vickers-indented brittle materials. In addition, however, surface chipping was observed outside the immediate indenter contact zone for the samples containing 50–70% porcellanite (Fig. 10(a)–(c)) but not for those containing 75–90% (Fig. 10(d)). This difference in response is most like linked to the differences in phases present and microstructures developed between the former and latter compositions.

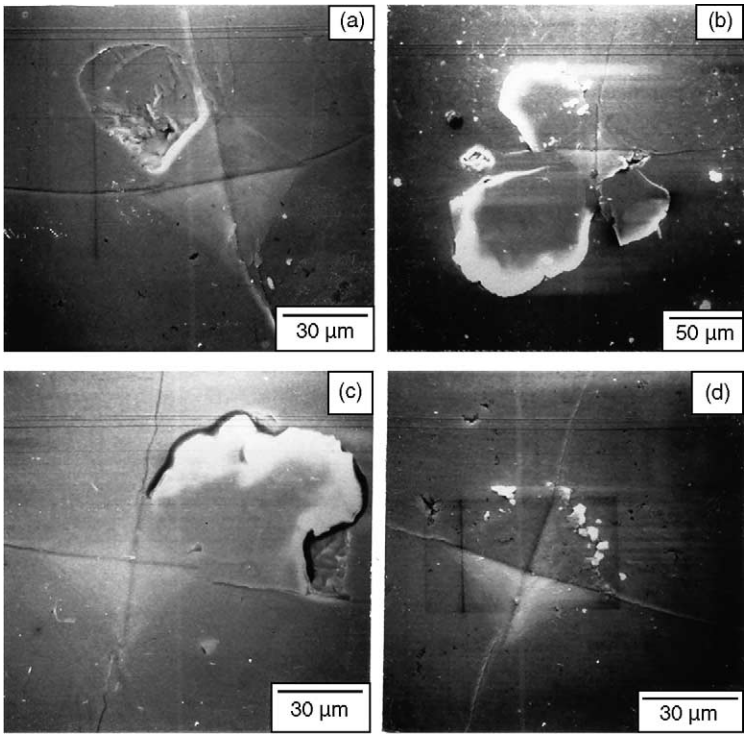

Fig. 10. Typical indenter contact response of samples originally containing: (a) 50%, (b) 60%, (c) 70% and (d) 80% porcellanite, respectively.

4. Conclusions

Compositions originally containing 50–90% porcellanite fused strongly and homogeneously, consequence of the presence of molten C_3S_2, a reaction product formed from lime and silica derived from the limestone and the porcellanite, respectively.

For the compositions originally containing 60 and 70% porcellanite, crystals of C_3AS_2 and C_2AS, formed as reaction products, are of thin, flat plate morphology. Further, embedded in C_3S_2, the crystals are randomly orientated and span a wide range of sizes.

C_3AS_2 and C_2AS do not form in samples for which the starting mix contained 75% and higher porcellanite. Instead, these microstructures feature C_3S_2-bonded long-fibre and/or particulate and dendtitic mullite, along with unreacted remnant silica.

Within the range of compositions over which strong fusing occurred, the sample originally containing 60% porcellanite exhibits highest microhardness. Further, samples for which the original mixes contained 50–70% porcellanite are more susceptible to extensive indenter contact damage than those originally containing 75–90%.

Acknowledgment

Caribbean Industrial Research Institute, Macoya, Trinidad and Tobago, kindly allowed the author use of its microhardness testing facility.

References

[1] J.C. Knight, High temperature reaction products in porcellanite–$CaCO_3$ mixtures, Ind. Ceram. 23 (1) (2004) 21–25.
[2] C.R. Bristow, Detail Survey of Part of the Trinidad Porcellanite Deposits, Overseas Division, Institute of Geological Surveys, London, 1969.
[3] L.C. Chadwick, Porcellanites from Trinidad, West Indies; Special Report 141, Overseas Geological Surveys, Mineral Reserve Division, London, 1969.
[4] J.C. Knight, High temperature thermochemical and thermophysical transformation of porcellanite, Br. Ceram. Trans. 101 (3) (2002) 125–128.